Published in final edited form as:
*Free Radic Biol Med*. 2008 April 1; 44(7): 1305–1313.

# Extracellular SOD protects the heart against oxidative stress and hypertrophy after myocardial infarction

**Elza D. van Deel**[*,1,2], **Zhongbing Lu**[*,1], **Xin Xu**[1], **Guangshuo Zhu**[1], **Xinli Hu**[1], **Tim D. Oury**[3], **Robert J Bache**[1], **Dirk J. Duncker**[2], and **Yingjie Chen**[1]

[1]*Center for Vascular Biology and Cardiovascular Division, Department of Medicine, University of Minnesota Medical School, Minneapolis, MN55455, USA* [2]*Division of Experimental Cardiology, Department of Cardiology, Thoraxcenter, Cardiovascular Research School COEUR, Erasmus MC, University Medical Center Rotterdam, P.O. Box 2040, 3000 CA, Rotterdam, The Netherlands* [3]*Department of Pathology, University of Pittsburgh Medical Center, University of Pittsburgh, Pittsburgh, Pennsylvania 15261, USA.*

## Abstract

Extracellular SOD (**EC-SOD**) contributes only a small fraction to total SOD activity in the heart, but is strategically located to scavenge free radicals in the extracellular compartment. EC-SOD expression is decreased in myocardial infarction (MI)-induced failing heart, but whether EC-SOD can abrogate oxidative stress or modify MI-induced ventricular remodeling has not been previously studied. Subsequently, the effect of EC-SOD gene deficiency (EC-SOD KO) on left ventricular (LV) oxidative stress, hypertrophy, and fibrosis were studied in EC-SOD KO and wild type mice under control conditions, 4 weeks and 8 weeks after permanent coronary artery ligation. EC-SOD KO had no detectable effect on LV function in normal hearts, but caused small but significant increases of LV fibrosis. Eight weeks after MI, EC-SOD KO mice developed significantly more LV hypertrophy (LV mass increased 1.64-fold in KO mice as compared to 1.35-fold in wild type mice, $p<0.01$), and more fibrosis and myocyte hypertrophy which was more prominent in the peri-infarct region than in the remote myocardium. EC-SOD KO mice had greater increases of nitrotyrosine in the peri-infarct myocardium, and this was associated with a greater reduction of LV ejection fraction, a greater decrease of Sarcoplasmic or Endoplasmic Reticulum Calcium 2 ATPase (SERCA2a) and a greater increase of atrial natriuretic peptide (ANP) in the peri-infarct zone compared to wild type mice. EC-SOD KO was associated with more increases of phosphorylated p38 (p-p38$^{Thr180/Tyr182}$), p42/44 extracellular signal-regulated kinase (p-Erk$^{Thr202/Tyr204}$) and c-Jun N-terminal kinase (p-JNK $^{Thr183/Tyr185}$) under both control conditions or after MI, indicating that EC-SOD KO increases activation of mitogen-activated protein kinase (MAPK) signaling pathways. These findings demonstrated that EC-SOD plays an important role in protecting the heart against oxidative stress and infarction induced ventricular hypertrophy.

### Keywords

oxygen radicals; infarction; hypertrophy; remodeling; extracellular matrix

Address for correspondence: Yingjie Chen, MD, PhD University of Minnesota Mayo Mail Cod 508 420 Delaware St. SE Minneapolis, MN55455 Tel: (612) 624-8970 Fax: (612) 626-4411 email: chenx106@tc.umn.edu.
*These authors contributed equally.

## Introduction

Left ventricular hypertrophy and dysfunction after myocardial infarction (MI) is associated with increased production of reactive oxygen species (ROS) and depressed antioxidant reserves, suggesting that oxidative stress might contribute to ventricular remodeling and the development of ventricular hypertrophy and congestive heart failure (CHF)[1]. Superoxide dismutase (SOD) is the first line of defense against ROS. Three SOD isozymes have been identified, including a copper/zinc-containing SOD (CuZn-SOD) which is primarily cytosolic in location, a mitochondrial manganese SOD (Mn-SOD), and extracellular SOD (EC-SOD). EC-SOD is a glycoprotein secreted into the extracellular fluid by cells such as fibroblast, endothelial cell and smooth muscles that binds to sulfated polysaccharides such as heparin and heparan sulfate[2,3] as well as other matrix components[4,5]. As a result, EC-SOD binds to the surface of endothelial cells and the extracellular matrix which has a high abundance of heparan sulfate [6]. Patients in whom EC-SOD binding to endothelial cells is decreased as the result of substitution of arginine-213 by glycine (R213G) have an increased incidence of hypertension[7] and increased risk of ischemic heart disease[7,8], implying that impaired EC-SOD binding or decreased myocardial EC-SOD content can increase the vulnerability to cardiovascular disease. Several recent studies have demonstrated that EC-SOD expression is decreased in the failing heart, and this was associated with evidence of increased myocardial oxidative stress and endothelial dysfunction[9-11]. However, whether EC-SOD can influence ventricular oxidative stress and remodeling after MI remains unknown. Here we examined the effect of EC-SOD gene deletion (EC-SOD$^{-/-}$) on myocardial oxidative stress and cardiac remodeling following MI. EC-SOD$^{-/-}$ had no effect on left ventricular (LV) function under normal conditions, but did result in slight but significant myocyte hypertrophy and myocardial fibrosis that was associated with activation of the mitogen-activated protein kinase (MAPK) signaling cascades. MI resulted in evidence of increased oxidative stress that was greater in the EC-SOD$^{-/-}$ mice, and was associated with more myocardial hypertrophy and fibrosis, as well as a more prominent decrease of ejection fraction than in the wild type mice. These findings provide the first direct evidence that EC-SOD exerts a significant protective effect against myocardial infarction induced oxidative stress and ventricular remodeling.

## Methods

### Mice

Male C57BL/6 (Taconic, Germantown, NY) and EC-SOD$^{-/-}$ mice (congenic with the Taconic C57BL/6 strain of mice[3,12]), 8–10 weeks of age, were used for study. The investigation conforms with the Guide for the Care and Use of Laboratory Animals published by the US National Institutes of Health (NIH Publication No. 85-23, revised 1996).

### Experimental procedure

MI was produced by permanent ligation of the left anterior descending coronary artery in wild type (n=33) and EC-SOD$^{-/-}$ mice (n=35). Mice were anesthetized and instrumented for hemodynamic measurements at four or eight weeks after MI. Body weight and age matched wild type mice (n=17) and EC-SOD$^{-/-}$ mice (n=22) were used as controls for functional analysis after sham surgery.

### Echocardiography

Mice were anesthetized with 1.5% isoflurane. Echocardiographic images were obtained with a Visualsonics high resolution Veve 660 system as previously described [13]. LV cross sectional area at end diastole ($LVCSA_d$) and at end systole ($LVCSA_s$), LV long axis diameter at end diastole ($LVD_d$) or at end systole ($LVD_s$), and LV short axis wall thickness were

measured. LV ejection fraction (LVEF) was calculated by the cubic method: LVEF= [( $LVCSA_d$) × ($LVD_d$) − ($LVCSA_s$) × ($LVD_s$)]/ ($LVCSA_d$) × ($LVD_d$) ×100%.

### Evaluation of aortic pressure and LV hemodynamics

The mice were weighed, anesthetized with 4% isoflurane, intubated using a 24G catheter and ventilated with a mouse ventilator (HSE Harvard Apparatus; Germany). The ventilation rate was set at 120 breaths per minute with a tidal volume of 250–300 μl and a positive end expiratory pressure of 4 cm $H_2O$. Animals were ventilated with a gas mixture of $O_2/N_2$ (1/2); anesthesia was maintained using 2.5% isoflurane and body temperature was maintained at 37° C by placing the mice on a temperature-controlled heating pad. For hemodynamic measurements, a 1.2F pressure catheter (Scisence Inc.; Ontario, Canada) was inserted in the right carotid artery to record aortic pressure and advanced into the LV to measure LV pressure, its first derivative (LV dP/dt) and heart rate (HR).

Hemodynamic data were digitized on-line and processed using IOX data acquisition and analysis software (EMKA technologies; Falls Church, USA). At least ten beats during stable hemodynamic conditions were collected for data analysis.

### Western blots

LV protein content was analyzed using Western blots as previously described (n=4 samples each group)[14]. Primary antibodies against CuZn-SOD, Mn-SOD, EC-SOD, atrial natriuretic peptide (ANP), Sarcoplasmic or Endoplasmic Reticulum Calcium 2 ATPase (SERCA2a), nitrotyrosine, total c-Jun N-terminal kinase (JNK), phosphorylated JNK (p-$JNK^{Thr183/Tyr185}$) and catalase were purchased from Transduction Laboratories, Santa Cruz Inc, Abcam Inc, Upstate and Sigma, respectively. The antibodies against phosphorylated p38 MAP kinase (p-$p38^{Thr180/Tyr182}$), p42/44 extracellular signal-regulated kinase (ERK), and phosphorylated p42/44 MAP kinase (p-$Erk^{Thr202/Tyr204}$) were purchased from Cell Signaling.

### SOD activity

Total SOD activity of LV homogenates was determined with a Superoxide Anion Detection kit (Calbiochem Company), according to the manufacturer's instructions, and expressed as scavenging ability of the homogenates on superoxide anion (n=5 samples each group).

### Histological staining and measurement of fibrosis

Frozen tissue sections (8μm) from the central portion of the LV were stained with H&E (Sigma) for overall morphology, Sirius Red for fibrosis, and FITC-conjugated wheat germ agglutinin (AF488, Invitrogen) to evaluate myocyte size. For mean myocyte size, the short axis diameter and cross sectional area of at least 120 cells/sample (from 4 areas) and at least 4 samples of each group were averaged. The percent volume fibrosis was determined using the method described in Unbiased Stereology[15].

### Data and Statistical Analyses

All values were expressed as mean ± standard error of the mean (SEM). Statistical significance was defined as $P < 0.05$. One-way analysis of variance (ANOVA) was used to test each variable for differences among the treatment groups with StatView (SAS Institute Inc). If the ANOVA demonstrated a significant effect, post hoc pairwise comparisons were made with Fisher's least significant difference test.

## Results

### EC-SOD$^{-/-}$ exacerbated MI-induced ventricular hypertrophy and fibrosis

Under control conditions, LV weight, and the ratio of LV weight to body weight (an index of ventricular hypertrophy) were slightly but significantly greater in the EC-SOD$^{-/-}$ mice as compared to wild type mice (Figure 1, Table 1). Eight weeks after MI we observed significant myocardial hypertrophy, as indicated by increases of ventricular weight and the ratio of ventricular weight to body weight or to tibia length, in both wild type and EC-SOD$^{-/-}$ mice, but the degree of hypertrophy was significantly greater in the EC-SOD$^{-/-}$ mice than in the wild type mice (Figure 1A, 1B, 1C). This was also true four weeks after MI (Table 1). Myocardial infarct size was not different between wild type and EC-SOD$^{-/-}$ mice (Table 1). The MI induced mortality was not different between EC-SOD$^{-/-}$ and wild type mice (8 of 33 wild type mice and 8 of 35 EC-SOD$^{-/-}$ mice died during the post MI period).

Histological staining of LV tissue was performed on EC-SOD$^{-/-}$ and wild type mice under control conditions and 8 weeks after MI. The EC-SOD$^{-/-}$ mice had slightly but significantly more fibrosis than the wild type mice under control conditions (Figure 2A, 2B). MI resulted in significant increases of fibrosis in both the peri-infarct and remote zones, and this was significantly greater in the EC-SOD$^{-/-}$ mice (Figure 2A,2B). MI caused myocyte hypertrophy in both the peri-infarct and remote zones that was significantly greater in the EC-SOD$^{-/-}$ mice than in the wild type mice (Figure 2A,2C). Thus, the greater ventricular mass in the EC-SOD$^{-/-}$ mice in response to MI was the result of increases of both myocyte size and ventricular fibrosis.

Aortic pressure, LV systolic pressure and LV $dP/dt_{max}$ were not different between wild type mice and EC-SOD$^{-/-}$ mice under control conditions. At both four and eight weeks after MI, we observed small but significant decreases of LV systolic pressure, mean aortic pressure, LV $dP/dt_{max}$ and LV $dP/dt_{min}$ in both wild type mice and EC-SOD$^{-/-}$ mice. MI for 4 and 8 weeks tended to cause greater decreases of LV $dP/dt_{max}$ and LV $dP/dt_{min}$ in EC-SOD$^{-/-}$ mice as compared with wild type mice, but these differences were not significant (Table 1). Echocardiographic imaging of the heart 8 weeks after MI demonstrated significant increases of LV cross sectional area at end diastole in both EC-SOD$^{-/-}$ and wild type mice in comparison with sham operated mice (Table 1, Figure 1E), indicating MI-induced LV dilation. The increase of LV cross sectional area at end diastole tended to be greater in the EC-SOD$^{-/-}$ mice than in the wild type mice ($p=0.06$). Eight weeks after MI, LV cross sectional area at end systole was significantly increased in both EC-SOD$^{-/-}$ and wild type mice in comparison with sham operated mice (Table 1, Figure 1E), but this increase was 19% greater ($p<0.05$) in the EC-SOD$^{-/-}$ mice than in the wild type mice, indicating that MI caused more ventricular remodeling in the EC-SOD$^{-/-}$ mice. However, LV cross sectional area at end diastole was also increased in the EC-SOD$^{-/-}$ mice, so that MI caused only a slightly greater decrease of LV ejection fraction in the EC-SOD$^{-/-}$ than in the wild type mice (Figure 1F, Table 1). Overall, the echocardiographic and LV pressure measurements demonstrated that EC-SOD$^{-/-}$ only moderately exacerbated the MI-induced LV dysfunction.

ANP is a sensitive biochemical marker for LV hypertrophy and/or ventricular remodeling. Myocardial ANP levels were increased in both wild type and EC-SOD$^{-/-}$ mice 8 weeks after MI; this increase was greater in the peri-infarct zone than the remote zone where it was significantly greater in the EC-SOD$^{-/-}$ mice than the wild type mice (Figure 3A, 3B). SERCA2a, which pumps calcium from the cytosol back into the sarcoplasmic reticulum at the end of systole, is generally decreased in the setting of heart failure. Under control conditions SERCA2A was significantly higher in EC-SOD$^{-/-}$ mice than in wild type mice. In the wild type mice SERCA2a was significantly increased in the remote zone 8 weeks after MI, but was unchanged in the peri-infarct zone. SERCA2a was significantly lower in both the remote and

the peri-infarct zones of the EC-SOD$^{-/-}$ mice as compared to wild type mice 8 weeks after MI (Figure 3A, 3C). Taken together, these data are consistent with more prominent myocardial hypertrophy and fibrosis in the EC-SOD$^{-/-}$ mice after MI.

### EC-SOD$^{-/-}$ exacerbated MI-induced myocardial oxidative stress

As anticipated, EC-SOD was undetectable in the EC-SOD$^{-/-}$ mice (Figure 4A, 4B). EC-SOD$^{-/-}$ did not affect myocardial CuZn-SOD or Mn-SOD protein content under control conditions (Figure 4A, 4C, 4D). Total myocardial SOD activity was not different between wild type mice and EC-SOD$^{-/-}$ mice under control conditions (Figure 4E), consistent with previous reports that EC-SOD contributes only minimally to overall myocardial SOD activity [2,16]. Myocardial nitrotyrosine content were not different between EC-SOD$^{-/-}$ mice and wild type mice under control conditions (Figure 3A, 3D). Myocardial catalase protein content was not different between wild type and EC-SOD$^{-/-}$ mice (Figure 4A, 4F) under control conditions.

MI caused significant increases of myocardial nitrotyrosine in both the remote and the peri-infarct zones of wild type and EC-SOD$^{-/-}$ mice, and these increases were significantly greater in the EC-SOD$^{-/-}$ mice than in the wild type mice (Figure 3A,3D), indicating increased myocardial oxidative stress in EC-SOD$^{-/-}$ mice after MI. SOD activity in the peri-infarct zone was significantly decreased in the EC-SOD$^{-/-}$ mice 8 weeks after MI, but not in the wild type mice (Figure 4E). Myocardial catalase protein content was not different between wild type and EC-SOD$^{-/-}$ mice during control conditions and did not change significantly after MI (Figure 4F).

### EC-SOD$^{-/-}$ alters activation of mitogen-activated protein kinases (MAPK)

MAPKs are major targets of reactive oxygen species [17], and the development of ventricular hypertrophy or heart failure is often associated with increased oxidative stress and activation of MAPK[18]. To understand whether EC-SOD$^{-/-}$ alters MAPK signaling in the normal or infarcted heart, total and phosphorylated p-38, JNK and ERK were determined (Figure 5). In control noninfarcted hearts EC-SOD$^{-/-}$ was associated with significant increases of p-p38$^{Thr180/Tyr182}$, p-Erk$^{Thr202/Tyr204}$ and p-JNK $^{Thr183/Tyr185}$ as well as the ratios of the phosphorylated to total proteins. MI caused significant increases of p-p38$^{Thr180/Tyr182}$ and p-JNK $^{Thr183/Tyr185}$ as well as the ratios of p-p38 to total p38, and p-JNK to total JNK in the remote zone; in the peri-infarct region the increase in p-JNK also occurred in both groups of animals, but the increase of p-p38 occurred only in the EC-SOD$^{-/-}$ animals. P-Erk$^{Thr202/Tyr204}$ increased following MI but, owing to an increase in total Erk, the ratio of p-Erk to total ERK was little changed in either the remote or peri-infarct zones (Figure 5).

## Discussion

The major new findings of this study are that (i) following MI EC-SOD$^{-/-}$ hearts sustained more hypertrophy and fibrosis than wild type hearts, with a greater increase of LV cross section at end systole and a greater decrease of LV ejection fraction; (ii) MI caused a greater increase in oxidative stress, as indicated by nitrotyrosine, in EC-SOD$^{-/-}$ hearts than in wild type hearts, and (iii) EC-SOD$^{-/-}$ resulted in activation of myocardial MAPK signaling pathways in both unstressed and infarcted hearts. To the best of our knowledge, these findings provide the first evidence that EC-SOD exerts a protective effect against MI-induced ventricular remodeling and modulates activation of the MAPK signaling pathway.

The unchanged myocardial SOD activity in the EC-SOD$^{-/-}$ mice under control conditions is consistent with previous reports that EC-SOD contributes minimally to overall SOD activity in the heart [2,16]. Nevertheless, the small, but significant, increase of myocardial fibrosis and ventricular mass, and activation of MAPK signaling pathways in the EC-SOD$^{-/-}$ mice under

control conditions, indicates that the loss of superoxide scavenging activity in the extracellular compartment has a significant influence on signaling related to myocyte hypertrophy and collagen deposition. The lack of change in myocardial nitrotyrosine content in the EC-SOD$^{-/-}$ mice under unstressed conditions may be accounted for by insufficient sensitivity of the assays for detecting small changes in these measurements. The increase of cardiac fibrosis in the EC-SOD$^{-/-}$ mice is analogous to previous reports that EC-SOD exerts anti-fibrotic activity in the lung [5,12]

The increases of nitrotyrosine in the mice subjected to MI in the present study are consistent with previous reports demonstrating increased oxidative stress in the failing heart [1,13,19, 20]. Thus, in animals with aortic constriction or MI, the development of heart failure was associated with increases of myocardial nitrotyrosine [13,20] and myocardial superoxide production [13,20,21]. Several sources for increased superoxide production have been identified in the failing heart, including the mitochondrial respiratory chain [22], uncoupled nitric oxide synthase [13,20], NADPH oxidase [23] and xanthine oxidase[24]. We recently reported that systolic overload produced by transverse aortic constriction in mice caused increased expression of the monomeric forms of myocardial iNOS and eNOS (a structure that generates superoxide rather than NO). Furthermore, iNOS deletion or selective pharmacologic inhibition of iNOS decreased markers of oxidative stress and improved LV function, suggesting that either iNOS-induced eNOS uncoupling or iNOS uncoupling contributed to the increased oxidative stress and development of CHF in the wild type mice [13,20]. Furthermore, administration of BH4 to prevent NOS uncoupling [20] or selective inhibition of xanthine oxidase or NADPH oxidase has been reported to attenuate oxidative stress and ventricular dysfunction in this model of cardiac overload.

In addition to increased free radical production in the failing heart, there is evidence that decreased antioxidant reserves contribute to increased oxidative stress. Thus, CHF is associated with decreased EC-SOD protein content or activity [9-11] and overexpression of EC-SOD has been reported to protect the heart against ischemia-reperfusion injury [25,26] (an effect not enhanced by administration of catalase, demonstrating that protection was dependent upon removal of superoxide but not hydrogen peroxide). In contrast to these previous reports in failing hearts, in the present study EC-SOD protein was significantly increased in the peri-infarct region, and SOD1 protein was increased in both the peri-infarct and remote regions of the infarcted hearts. The failure to find decreases of SOD protein in the present study likely occurred because the animals were studied relatively early, when LV dysfunction produced by MI had not yet resulted in congestive heart failure.

Nevertheless, we did find a small but significant decrease of SOD activity in the peri-infarct region of the EC-SOD$^{-/-}$ mice after MI, with no change in the remote region. This decrease of SOD activity limited to the peri-infarct zone is consistent with previous reports of myocardial infarct in rats [27]. Furthermore, myocyte hypertrophy and fibrosis were more prominent in the peri-infarct region than in the remote myocardium. This greater structural abnormality was not likely the result of ischemia in the peri-infarct region, since the perfusion boundary between adjacent coronary perfusion beds has a sharp transition from hypoperfusion in the infarct region to normal perfusion in the adjacent myocardium [28]. However, local activation of stretch activated signaling could explain the greater hypertrophy and fibrosis in the peri-infarct region. Tethering of the noncontractile infarct to adjacent viable myocardium amplifies wall stresses in the peri-infarct region, and biomechanical strain can trigger stretch activated signaling pathways in cardiomyocytes [29]. This might also account for the significantly greater increase of ANP protein in the peri-infarct region compared to the remote region. The concept that stretch activated signaling pathways can be turned on regionally is supported by studies in rats 6 weeks post-infarction where substantial differences in mRNA levels for ANP, endothelin-1 and IGF-1 were found between the peri-infarct zone and the remote myocardium [30], with

highest expression in regions that were subjected to high mechanical stresses. The findings of evidence for increased oxidative stress, fibrosis, myocyte hypertrophy and increased ANP expression in the peri-infarct zone are similar to findings in the myocardium of hearts with overt heart failure. These findings are of interest because of evidence that the peri-infarct region can progressively expand over time and thereby contribute to the transition from compensated hypertrophy to heart failure [31]. Thus, with sufficient time, it is possible that the remote zone would gradually take on characteristics seen in the peri-infarct region. This evolution toward heart failure appeared more prominent in the EC-SOD$^{-/-}$ mice, where the degree of ventricular hypertrophy was significantly greater at 8 weeks post infarct than at 4 weeks, than in the wild type mice which showed no increase in hypertrophy between 4 and 8 weeks post infarct.

The MAPK cascades (in which MAPKs are activated by phosphorylation by upstream MAPK kinases) are important regulatory pathways in cardiac pathophysiology[32,33]. The most widely investigated MAPKs in the heart are the ERK1/2, JNKs and p38-MAPKs. ROS are known to activate myocardial MAPK signaling pathways, and reducing oxidative stress attenuates MAPK signaling [34-36]. In the present study, the increases of p-p38$^{Thr180/Tyr182}$, p-ERK$^{Thr202/Tyr204}$ and p-JNK $^{Thr183/Tyr185}$ in the EC-SOD$^{-/-}$ hearts during control conditions, compared with the wild type hearts, suggests that increased oxidative stress in the EC-SOD$^{-/-}$ hearts was able to activate these pathways even during unstressed conditions. ERK1/2 are activated by oxidative stress in cardiac myocytes [35-37]. Constitutive activation of ERK1/2 by cardiac specific overexpression of their upstream regulator MAPK kinase 1 [38,39] or RAS[40] results in ventricular hypertrophy or congestive heart failure, indicating that activation of the ERK signaling pathway causes ventricular hypertrophy. ROS also activates p38 and JNK [35,36]. Activation of p38 by TAK1 induced ventricular hypertrophy [41]. Tenhunen et al [42] injected adenovirus encoding wild-type p38-MAPKα together with a constitutively-activated upstream kinase into the hearts of rats; the hearts overexpressing p38 MAPK had increased expression of genes related to cell cycle progression and inflammation together with large areas of fibrosis. This observation, which is consistent with the established link between the p38 MAPK pathway and inflammatory responses in other organ systems, is similar to the findings in the peri-infarct region in the present study. In addition, specific activation of JNKs by overexpression of activated MKK3 or MKK6 induces ventricular dilation and congestive heart failure [43]. Taken together, these findings suggest that activation of the MAPK signaling pathway as the result of increased myocardial oxidative stress in EC-SOD$^{-/-}$ mice in the present study may have contributed to the myocyte hypertrophy, fibrosis or dysfunction observed in this strain both under control conditions and after MI.

In summary, EC-SOD$^{-/-}$ caused slight but significant myocyte hypertrophy and fibrosis in the unstressed heart that was associated with activation of the MAPK signaling pathway. In response to coronary occlusion, EC-SOD$^{-/-}$ mice developed more LV hypertrophy than wild type mice, with a greater decrease of ejection fraction. The degree of fibrosis and myocyte hypertrophy was significantly greater in the peri-infarct region of the EC-SOD$^{-/-}$ mice than in the wild type mice, and this was associated with significantly greater ANP protein and significantly less SERCA2a, implying greater dysfunction in this region of the EC-SOD$^{-/-}$ mice. The data indicate that EC-SOD plays an important role in protecting the heart against oxidative stress and infarction induced ventricular hypertrophy.

**Acknowledgments**

We are grateful to Dr Stefan Marklund of Umea University, Umea, Sweden, for supply of breeding pairs of EC-SOD$^{-/-}$ mice.

Sources of Funding

This study was supported by NHLBI Grants HL71790 (YC), HL21872 (RJB), and HL63700 (TDO) from the National Institutes of Health.

## Abbreviations

ANP, atrial natriuretic peptide
CHF, congestive heart failure
CuZn-SOD, copper/zinc-containing superoxide dismutase
EC-SOD, extracellular superoxide dismutase
ERK, extracellular signal-regulated kinase
JNK, c-Jun N-terminal kinase
LV, left ventricular
MAPK, mitogen-activated protein kinase
MI, myocardial infarction
Mn-SOD, manganese superoxide dismutase
ROS, reactive oxygen species
SERCA2a, Sarcoplasmic or endoplasmic reticulum calcium 2 ATPase

## Reference List


1. Giordano FJ. Oxygen, oxidative stress, hypoxia, and heart failure. J Clin Invest 2005;115:500–508. [PubMed: 15765131]
2. Marklund SL. Extracellular superoxide dismutase and other superoxide dismutase isoenzymes in tissues from nine mammalian species. Biochem. J 1984;222:649–655. [PubMed: 6487268]
3. Carlsson LM, Jonsson J, Edlund T, Marklund SL. Mice lacking extracellular superoxide dismutase are more sensitive to hyperoxia. Proc. Natl. Acad Sci U. S. A 1995;92:6264–6268. [PubMed: 7603981]
4. Petersen SV, Oury TD, Ostergaard L, Valnickova Z, Wegrzyn J, Thogersen IB, Jacobsen C, Bowler RP, Fattman CL, Crapo JD, Enghild JJ. Extracellular superoxide dismutase (EC-SOD) binds to type i collagen and protects against oxidative fragmentation. J Biol. Chem 2004;279:13705–13710. [PubMed: 14736885]
5. Fattman CL, Schaefer LM, Oury TD. Extracellular superoxide dismutase in biology and medicine. Free Radic. Biol. Med 2003;35:236–256. [PubMed: 12885586]
6. Sandstrom J, Carlsson L, Marklund SL, Edlund T. The heparin-binding domain of extracellular superoxide dismutase C and formation of variants with reduced heparin affinity. J Biol. Chem 1992;267:18205–18209. [PubMed: 1517248]
7. Juul K, Tybjaerg-Hansen A, Marklund S, Heegaard NH, Steffensen R, Sillesen H, Jensen G, Nordestgaard BG. Genetically reduced antioxidative protection and increased ischemic heart disease risk: The Copenhagen City Heart Study. Circulation 2004;109:59–65. [PubMed: 14662715]
8. Yamada H, Yamada Y, Adachi T, Fukatsu A, Sakuma M, Futenma A, Kakumu S. Protective role of extracellular superoxide dismutase in hemodialysis patients. Nephron 2000;84:218–223. [PubMed: 10720891]
9. Chen Y, Hou M, Li Y, Traverse JH, Zhang P, Salvemini D, Fukai T, Bache RJ. Increased superoxide production causes coronary endothelial dysfunction and depressed oxygen consumption in the failing heart. Am J Physiol Heart Circ Physiol 2005;288:H133–H141. [PubMed: 15598865]
10. Landmesser U, Merten R, Spiekermann S, Buttner K, Drexler H, Hornig B. Vascular extracellular superoxide dismutase activity in patients with coronary artery disease: relation to endothelium-dependent vasodilation. Circulation 2000;101:2264–2270. [PubMed: 10811593]
11. Landmesser U, Spiekermann S, Dikalov S, Tatge H, Wilke R, Kohler C, Harrison DG, Hornig B, Drexler H. Vascular oxidative stress and endothelial dysfunction in patients with chronic heart failure: role of xanthine-oxidase and extracellular superoxide dismutase. Circulation 2002;106:3073–3078. [PubMed: 12473554]
12. Fattman CL, Tan RJ, Tobolewski JM, Oury TD. Increased sensitivity to asbestos-induced lung injury in mice lacking extracellular superoxide dismutase. Free Radic. Biol. Med 2006;40:601–607. [PubMed: 16458190]
13. Zhang P, Xu X, Hu X, van Deel ED, Zhu G, Chen Y. Inducible nitric oxide synthase deficiency protects the heart from systolic overload-induced ventricular hypertrophy and congestive heart failure. Circ Res 2007;100:1089–1098. [PubMed: 17363700]

14. Chen Y, Li Y, Zhang P, Traverse JH, Hou M, Xu X, Kimoto M, Bache RJ. Dimethylarginine dimethylaminohydrolase and endothelial dysfunction in failing hearts. Am J Physiol Heart Circ Physiol 2005;289:H2212–H2219. [PubMed: 16024577]
15. Howard, CV.; Reed, MG. Estimation of component volume and volume fraction. In: Catherine, J., editor. Unbiased Stereology, Three-dimensional measurement in microscopy. BIOS Scientific Publishers; Abingdon, Oxon: 2005. p. 17-64.
16. Marklund SL. Extracellular superoxide dismutase in human tissues and human cell lines. J Clin Invest 1984;74:1398–1403. [PubMed: 6541229]
17. Das DK, Maulik N, Engelman RM. Redox regulation of angiotensin II signaling in the heart. J Cell Mol. Med 2004;8:144–152. [PubMed: 15090271]
18. Heineke J, Molkentin JD. Regulation of cardiac hypertrophy by intracellular signalling pathways. Nat Rev Mol. Cell Biol 2006;7:589–600. [PubMed: 16936699]
19. Dhalla AK, Singal PK. Antioxidant changes in hypertrophied and failing guinea pig hearts. Am J Physiol 1994;266:H1280–H1285. [PubMed: 8184905]
20. Takimoto E, Champion HC, Li M, Ren S, Rodriguez ER, Tavazzi B, Lazzarino G, Paolocci N, Gabrielson KL, Wang Y, Kass DA. Oxidant stress from nitric oxide synthase-3 uncoupling stimulates cardiac pathologic remodeling from chronic pressure load. J Clin Invest 2005;115:1221–1231. [PubMed: 15841206]
21. Jacob MH, Pontes MR, Araujo AS, Barp J, Irigoyen MC, Llesuy SF, Ribeiro MF, Bello-Klein A. Aortic-banding induces myocardial oxidative stress and changes in concentration and activity of antioxidants in male Wistar rats. Life Sci 2006;79:2187–2193. [PubMed: 16956625]
22. Ide T, Tsutsui H, Kinugawa S, Utsumi H, Kang D, Hattori N, Uchida K, Arimura K, Egashira K, Takeshita A. Mitochondrial electron transport complex I is a potential source of oxygen free radicals in the failing myocardium. Circ Res 1999;85:357–363. [PubMed: 10455064]
23. Gupte SA, Levine RJ, Gupte RS, Young ME, Lionetti V, Labinskyy V, Floyd BC, Ojaimi C, Bellomo M, Wolin MS, Recchia FA. Glucose-6-phosphate dehydrogenase-derived NADPH fuels superoxide production in the failing heart. J Mol. Cell Cardiol 2006;41:340–349. [PubMed: 16828794]
24. Berry CE, Hare JM. Xanthine oxidoreductase and cardiovascular disease: molecular mechanisms and pathophysiological implications. J Physiol 2004;555:589–606. [PubMed: 14694147]
25. Li Q, Bolli R, Qiu Y, Tang XL, Murphree SS, French BA. Gene therapy with extracellular superoxide dismutase attenuates myocardial stunning in conscious rabbits. Circulation 1998;98:1438–1448. [PubMed: 9760299]
26. Iida S, Chu Y, Francis J, Weiss RM, Gunnett CA, Faraci FM, Heistad DD. Gene transfer of extracellular superoxide dismutase improves endothelial function in rats with heart failure. Am J Physiol Heart Circ Physiol 2005;289:H525–H532. [PubMed: 16014615]
27. Hill MF, Singal PK. Antioxidant and oxidative stress changes during heart failure subsequent to myocardial infarction in rats. Am J Pathol 1996;148:291–300. [PubMed: 8546218]
28. Factor SM, Sonnenblick EH, Kirk ES. The histologic border zone of acute myocardial infarction--islands or peninsulas? Am J Pathol 1978;92:111–124. [PubMed: 686143]
29. Jackson BM, Gorman JH III, Salgo IS, Moainie SL, Plappert T, St J, Edmunds LH Jr. Gorman RC. Border zone geometry increases wall stress after myocardial infarction: contrast echocardiographic assessment. Am J Physiol Heart Circ Physiol 2003;284:H475–H479. [PubMed: 12414441]
30. Loennechen JP, Stoylen A, Beisvag V, Wisloff U, Ellingsen O. Regional expression of endothelin-1, ANP, IGF-1, and LV wall stress in the infarcted rat heart. Am J Physiol Heart Circ Physiol 2001;280:H2902–H2910. [PubMed: 11356651]
31. Jackson BM, Gorman JH, Moainie SL, Guy TS, Narula N, Narula J, John-Sutton MG, Edmunds LH Jr. Gorman RC. Extension of borderzone myocardium in postinfarction dilated cardiomyopathy. J Am Coll. Cardiol 2002;40:1160–1167. [PubMed: 12354444]
32. Heineke J, Molkentin JD. Regulation of cardiac hypertrophy by intracellular signalling pathways. Nat Rev Mol. Cell Biol 2006;7:589–600. [PubMed: 16936699]
33. Clerk A, Cullingford TE, Fuller SJ, Giraldo A, Markou T, Pikkarainen S, Sugden PH. Signaling pathways mediating cardiac myocyte gene expression in physiological and stress responses. J Cell Physiol 2007;212:311–322. [PubMed: 17450511]

34. Sano M, Fukuda K, Sato T, Kawaguchi H, Suematsu M, Matsuda S, Koyasu S, Matsui H, Yamauchi-Takihara K, Harada M, Saito Y, Ogawa S. ERK and p38 MAPK, but not NF-kappaB, are critically involved in reactive oxygen species-mediated induction of IL-6 by angiotensin II in cardiac fibroblasts. Circ Res 2001;89:661–669. [PubMed: 11597988]

35. Yoshizumi M, Tsuchiya K, Tamaki T. Signal transduction of reactive oxygen species and mitogen-activated protein kinases in cardiovascular disease. J Med Invest 2001;48:11–24. [PubMed: 11286012]

36. Tanaka K, Honda M, Takabatake T. Redox regulation of MAPK pathways and cardiac hypertrophy in adult rat cardiac myocyte. J Am Coll. Cardiol 2001;37:676–685. [PubMed: 11216996]

37. Aikawa R, Komuro I, Yamazaki T, Zou Y, Kudoh S, Tanaka M, Shiojima I, Hiroi Y, Yazaki Y. Oxidative stress activates extracellular signal-regulated kinases through Src and Ras in cultured cardiac myocytes of neonatal rats. J Clin Invest 1997;100:1813–1821. [PubMed: 9312182]

38. Sugden PH, Clerk A. Cellular mechanisms of cardiac hypertrophy. J Mol. Med 1998;76:725–746. [PubMed: 9826118]

39. Bueno OF, Molkentin JD. Involvement of extracellular signal-regulated kinases 1/2 in cardiac hypertrophy and cell death. Circ Res 2002;91:776–781. [PubMed: 12411391]

40. Hunter JJ, Tanaka N, Rockman HA, Ross J Jr. Chien KR. Ventricular expression of a MLC-2v-ras fusion gene induces cardiac hypertrophy and selective diastolic dysfunction in transgenic mice. J Biol. Chem 1995;270:23173–23178. [PubMed: 7559464]

41. Zhang D, Gaussin V, Taffet GE, Belaguli NS, Yamada M, Schwartz RJ, Michael LH, Overbeek PA, Schneider MD. TAK1 is activated in the myocardium after pressure overload and is sufficient to provoke heart failure in transgenic mice. Nat Med 2000;6:556–563. [PubMed: 10802712]

42. Tenhunen O, Rysa J, Ilves M, Soini Y, Ruskoaho H, Leskinen H. Identification of cell cycle regulatory and inflammatory genes as predominant targets of p38 mitogen-activated protein kinase in the heart. Circ Res 2006;99:485–493. [PubMed: 16873723]

43. Liao P, Georgakopoulos D, Kovacs A, Zheng M, Lerner D, Pu H, Saffitz J, Chien K, Xiao RP, Kass DA, Wang Y. The in vivo role of p38 MAP kinases in cardiac remodeling and restrictive cardiomyopathy. Proc. Natl. Acad Sci U. S. A 2001;98:12283–12288. [PubMed: 11593045]

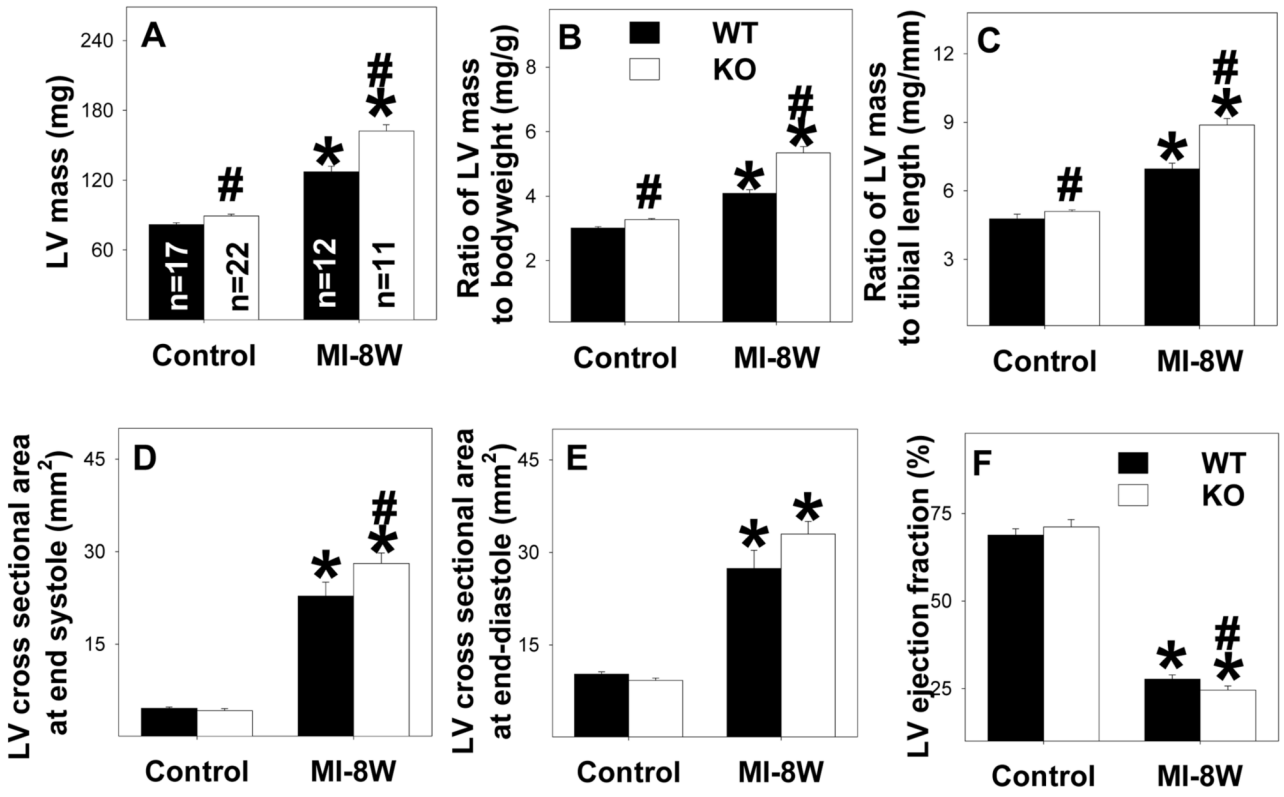


**Figure 1.**

EC-SOD$^{-/-}$ exacerbates MI-induced LV hypertrophy (A-C), dilatation (D-E) and decreased ejection fraction (F) 8 weeks following MI. *p<0.05 compared to the corresponding control mice; #p<0.05 compared to Wt mice.

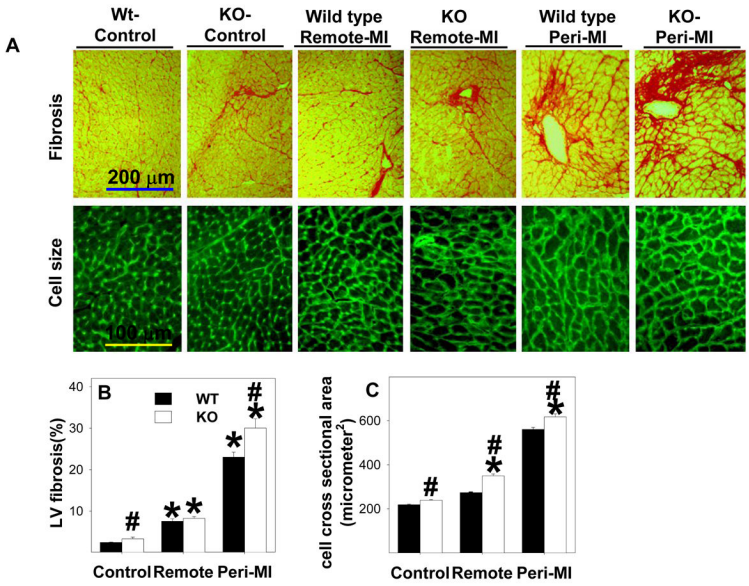


**Figure 2.**

EC-SOD$^{-/-}$ mice have increased myocardial fibrosis (A,B) and cardiac myocyte hypertrophy (A, C) during control conditions and following MI. *p<0.05 compared to the corresponding control mice; #p<0.05 compared to the corresponding Wt mice.

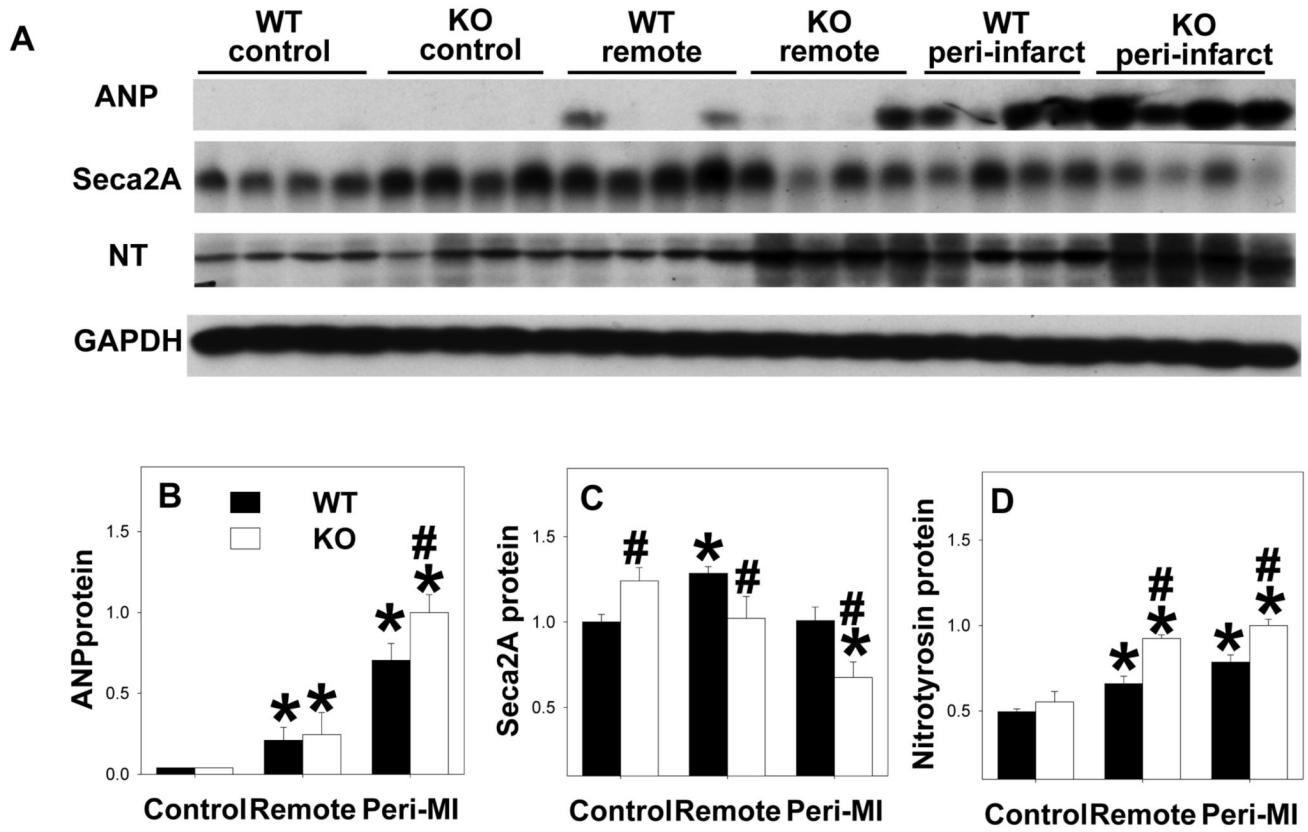


**Figure 3.**

EC-SOD$^{-/-}$ exacerbated the MI-induced increase of ventricular ANP in the peri-infarct zone (A,B), and the increase of nitrotyrosine in both the peri-infarct and remote zones (A,D). MI resulted in decreases of SERCA2a in the EC-SOD$^{-/-}$ mice but not in wild type mice (C). All data are expressed as arbitrary unit. *p<0.05 compared to the corresponding control; #p<0.05 compared to Wt-MI.

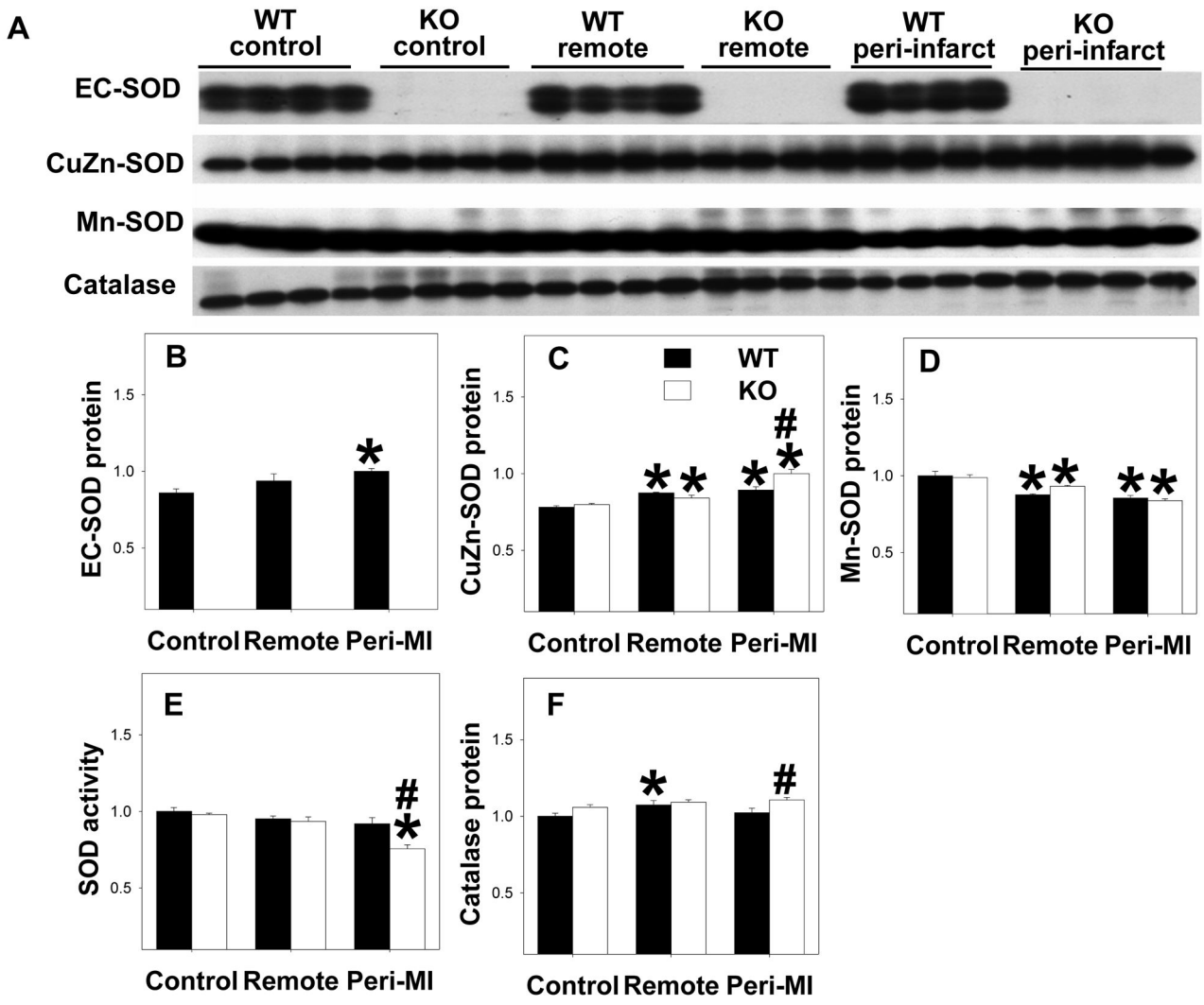


**Figure 4.**

Alterations of myocardial SOD protein content (A-D) and activity (E), and catalase content (F) under control conditions and 8 weeks after MI. All data are expressed as arbitrary unit. *p<0.05 compared to the corresponding control; #p<0.05 compared to Wt-MI.

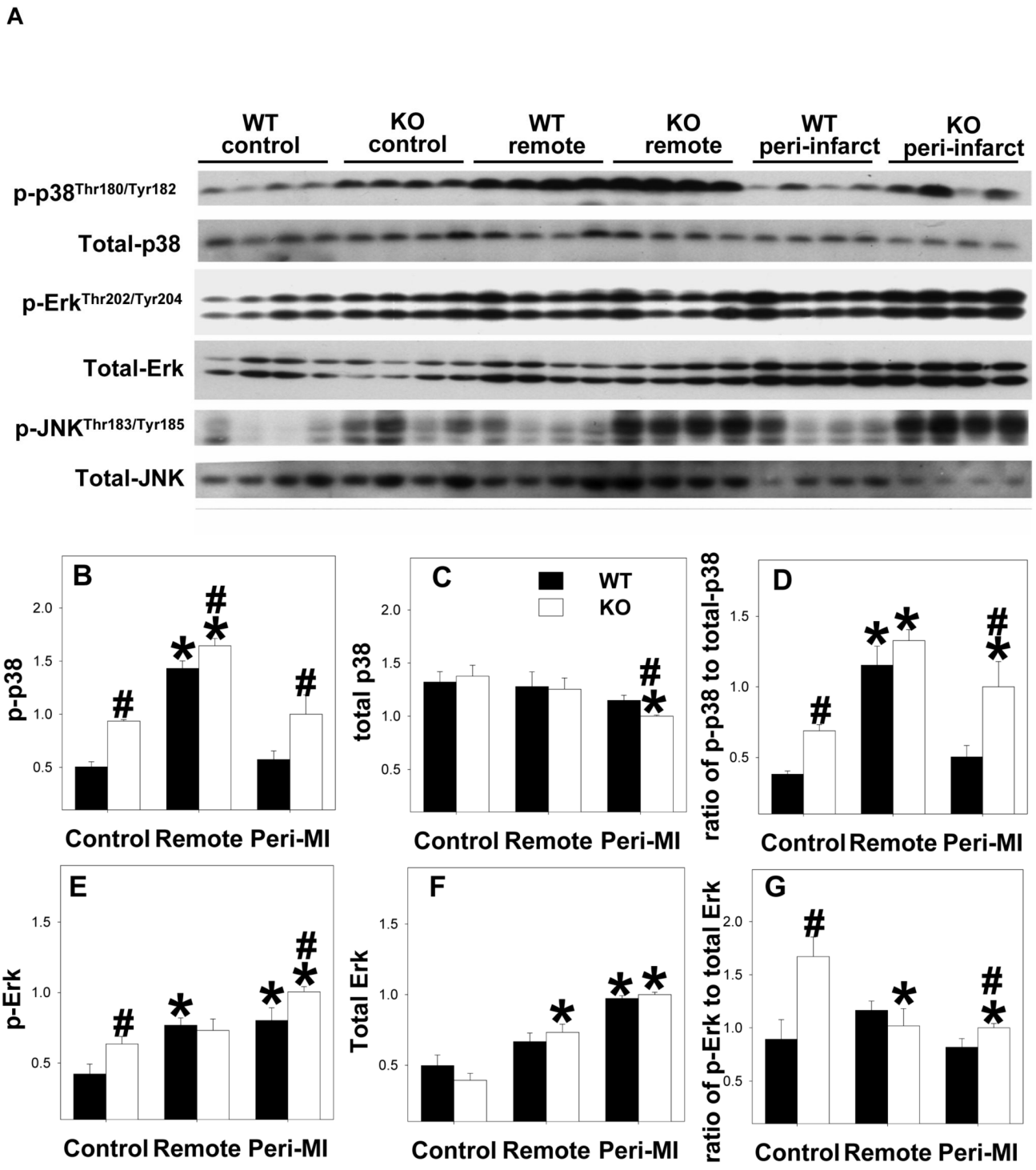

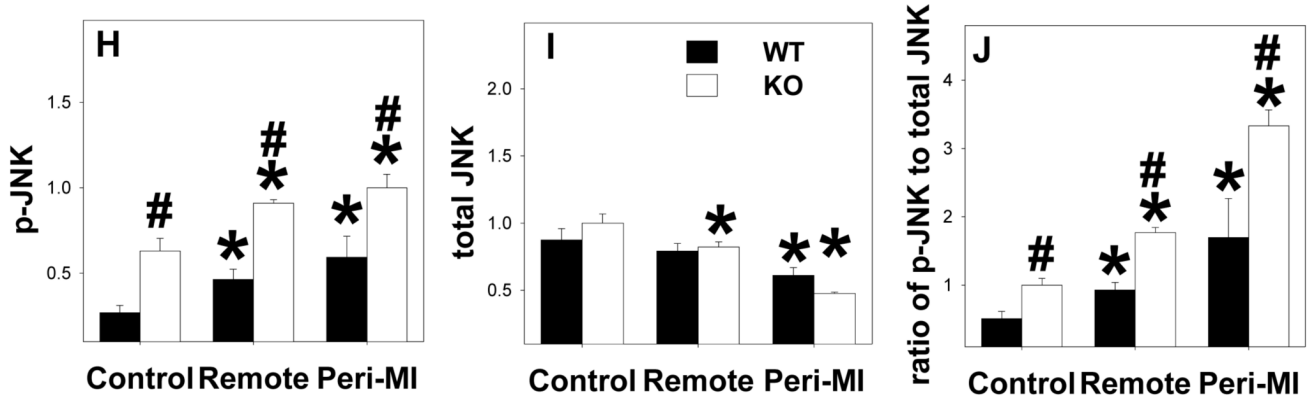


**Figure 5.**
P-p38$^{Thr180/Tyr182}$, total-p38, p-Erk$^{Thr202/Tyr204}$, total-Erk, p-JNK $^{Thr183/Tyr185}$ and total-JNK in EC-SOD$^{-/-}$ mice and wild type mice under control conditions and 8 weeks after MI. *p<0.05 compared to the corresponding control; #p<0.05 compared to Wt-MI.

**Table 1**

Anatomic and functional data for wild type (Wt) and EC-SOD−/− (KO) mice during control conditions and 4 weeks or 8 weeks after myocardial infarction.

| Parameters | Strain | Control | MI-4 weeks | MI-8 weeks |
|---|---|---|---|---|
| Body weight (g) | Wt | 28.1 ± 0.84 | 29.7 ± 1.5 | 31.1 ± 0.68 * |
| | KO | 28.0 ± 0.54 | 29.9 ± 0.87 | 30.5 ± 0.68 * |
| Heart mass (mg) | Wt | 105 ± 2.2 | 153 ± 7.0 * | 160 ± 6.0 * |
| | KO | 115 ± 2.3# | 185 ± 13 *# | 201 ± 7.0 *# |
| Ratio of heart mass to body weight (mg/g) | Wt | 3.9 ± 0.04 | 5.3 ± 0.27 * | 5.1 ± 0.16 * |
| | KO | 4.2 ± 0.04# | 6.2 ± 0.44 *# | 6.6 ± 0.24 *# |
| Heart mass/tibia length (mg/mm) | Wt | 6.2 ± 0.25 | 8.7 ± 0.42 * | 8.8 ± 0.33 * |
| | KO | 6.4 ± 0.11 | 10.0 ± 0.65 *# | 11.0 ± 0.37 *# |
| LV posterior wall thickness at end diastole (mm) | Wt | 0.65 0.01 | NA | 1.0 ± 0.04 * |
| | KO | 0.73 0.01 | NA | 0.99 ± 0.02 * |
| LV posterior wall thickness at end systole (mm) | Wt | 0.95 0.01 | NA | 1.2 ± 0.03 * |
| | KO | 0.98 0.14 | NA | 1.3 ± 0.02 *# |
| Heart rate (bpm) | Wt | 506 ± 14 | 503 ± 14 | 516 ± 16 |
| | KO | 513 ± 19 | 481 ± 9.8 | 503 ± 13 |
| Mean aortic pressure (mmHg) | Wt | 75 ± 2.8 | 69 ± 4.3 * | 65 ± 2.5 * |
| | KO | 77 ± 2.6 | 75 ± 2.7 * | 65 ± 2.2 * |
| LV systolic pressure (mmHg) | Wt | 96 ± 2.0 | 85 ± 4.2 * | 82 ± 2.9 * |
| | KO | 97 ± 2.6 | 88 ± 2.5 * | 83 ± 2.5 * |
| LV end diastolic pressure (mmHg) | Wt | 7.5 ± 1.5 | 11.4 ± 3.4 * | 12.2 ± 2.5 * |
| | KO | 6.6 ± 0.8 | 12.9 ± 2.3 * | 12.1 ± 3.5 * |
| LV $dP/dt_{max}$ (mmHg/s) | Wt | 8341 ± 377 | 5545 ± 691 * | 5090 ± 423 * |
| | KO | 7809 ± 612 | 4626 ± 305 * | 4536 ± 432 * |
| LV $dP/dt_{min}$ (mmHg/s) | Wt | −6739 ± 576 | −4983 ± 491 * | −4542 ± 387 * |
| | KO | −6833 ± 366 | −4140 ± 250 * | −4214 ± 471 * |
| Infarct area | Wt | 0% | 41.3 ± 1.6 * | 37.5 ± 2.3 * |
| | KO | 0% | 40.0 ± 1.3 * | 37.7 ± 0.78 * |

NA: not available.

* $p<0.05$ as compared with corresponding control conditions;

# $p<0.05$ as compared with wild type mice.